applied sciences

MDPI

Article

Combining High-Frequency GPR, Laser Scanning, and Digital Photogrammetry to Guide the Detachment of a Roman Mosaic in the Latomia dei Niccolini in Marsala (Italy)

Alessandra Carollo [1,*], Patrizia Capizzi [1], Raffaele Martorana [1], Alessandro Abrignani [2], Angelina Castiglia [3] and Mauro Lo Brutto [4]

[1] Department of Earth and Marine Sciences (DiSTeM), University of Palermo, 90123 Palermo, Italy; patrizia.capizzi@unipa.it (P.C.); raffaele.martorana@unipa.it (R.M.)
[2] Archaeological Association of the Ancient Mediterranean (AAMA), 91025 Marsala, Italy; abrignanialessandro@gmail.com
[3] PROPERART Cooperative Company, 94100 Enna, Italy; angelinacastiglia@properart.it
[4] Department of Engineering, University of Palermo, 90128 Palermo, Italy; mauro.lobrutto@unipa.it
* Correspondence: alessandra.carollo02@unipa.it

Abstract

This study presents the diagnostic and conservation work carried out on the Roman mosaic of the South cubiculum in the Latomia dei Niccolini (Marsala, western Sicily). The mosaic, decorated with polychrome tesserae featuring a kantharos motif, presented severe structural damage, including fractures, subsurface voids, and progressive material loss. To assess the causes of deterioration and design an effective conservation strategy, an integrated approach combining non-invasive geophysical and 3D survey methods was applied. Ground-penetrating radar (GPR) was selected as the main diagnostic tool because it allows high-resolution subsurface imaging while preserving the integrity of the fragile mosaic surface. By utilizing high-frequency 2 GHz antennas and complementary video inspection, a significant subsurface cavity beneath the mosaic preparation layer was successfully mapped, determining its critical relationship with the main diagonal surface fracture. Simultaneously, laser scanning and close-range photogrammetry enabled the creation of accurate 3D models supporting both documentation and restoration planning. The conservation concluded with surface cleaning, mortar consolidation, and the successful structural detachment and relocation of the compromised section onto a lightweight support for future museum display. The findings demonstrate that integrating 3D digital and geophysical data provides a quantitative, low-risk roadmap for preserving highly vulnerable archaeological floorings, moving beyond qualitative technical documentation to establish a replicable preservation framework.

Keywords: ground-penetrating radar; 3D survey; photogrammetry; laser scanning; 3D modeling; archaeological restoration; mosaic conservation; cultural heritage diagnostics

Check for updates

Academic Editor: Atsushi Mase

Received: 13 May 2026
Revised: 10 June 2026
Accepted: 12 June 2026
Published: 16 June 2026

1. Introduction

The investigation of ancient Roman mosaics often entails the use of integrated documentation and diagnostic methodologies, which are essential for the development of effective conservation strategies and for ensuring their accessibility and sustainable use. In particular, when ancient mosaics need to be detached and relocated, the knowledge of the mosaic and site conditions becomes fundamental.

Roman mosaics are often distinctive features of ancient Roman domus, but their presence can also characterize archaeological sites in different contexts. For instance, mosaics may be found in areas originally exploited as Latomiae (stone quarries) and subsequently reconfigured into necropolises or ancient cult areas.

Latomies are ancient stone quarries that hold historical and archaeological importance. These quarries played a crucial role in the construction and development of the ancient Greek and Roman cities, although they are not only quarries but often served multiple purposes [1]. Latomies were used for extracting limestone and calcarenite stones but also served as burial sites or were converted into amphitheaters and theaters. The archaeological remains in these quarries include evidence of the extraction process, inscriptions, and sometimes architectural features typical of burial complexes such as arcosolia, niches, and wall niches. Many of these quarries are open to the public and have become popular tourist attractions, allowing visitors to explore the ancient workings, learn about the historical context, and appreciate the architectural and engineering feats of the ancient Greeks and Romans. The preservation of these sites is a constant challenge due to factors such as weathering, human activity, and environmental impact. Conservation efforts aim to protect these historical treasures for future generations.

Latomies are relatively frequent in the archaeological areas of the Sicilian territory, and in some cases, they constitute unique and particular situations. Among these, the Latomia dei Niccolini represents important evidence in western Sicily. The Latomia dei Niccolini complex consists of ancient stone quarries situated at the edge of the Punic and Roman necropolis, to the east of the ancient city of Lilibeum, corresponding to present-day Marsala in western Sicily. The site is in the south-eastern sector of the urban area of Marsala, adjacent to the municipal cemetery, and constitutes an integral part of the Archaeological Park of Lilibeo-Marsala (Figure 1). The construction of the modern cemetery along the eastern edge of the Latomia, a long period of abandonment, and subsequent quarrying activities have seriously compromised the state of conservation of the tombs and destroyed valuable frescoes. The most significant element of the funerary system is the so-called South cubiculum, characterized by a small polychrome mosaic depicting a kantharos with flowing water, created with turquoise glass paste tiles. The floor mosaic, already at the time of its discovery, had a significant lesion that extended diagonally across a good part of the mosaic. This injury is probably caused by a large fracture whose rejection has progressively increased over time, resulting in a worsening of the mosaic's conditions, with degradation phenomena and tile loss.

To avoid further degradation, the Archaeological Park of Lilibeo-Marsala has planned digital documentation, geophysical investigation, and the restoration and consolidation of the mosaic. Furthermore, after consolidation, the detachment of the part that has fallen and its relocation to a new support at the Archaeological Museum of the Park was also planned. To this end, multidisciplinary diagnostic investigations necessary for a better understanding of the causes of the fracture and the differential settlements of the entire structure were carried out; these investigations have proven to be preparatory to the resolution of the problems that have caused the damage.

To evaluate the site conditions and the actual state of the Roman mosaic, an in-depth archaeological study was initially conducted, followed by a comprehensive 3D survey and a high-frequency ground-penetrating radar (GPR) investigation of the flooring. While the separate applications of GPR and 3D digital photogrammetry are increasingly documented in cultural heritage diagnostics, a major literature gap remains regarding their dynamic integration into an operational feedback loop capable of guiding high-risk structural interventions on highly fragile, subsurface compromised Roman mosaics. In most conventional conservation projects, geophysical data serves merely as preliminary qualitative diagnostics. To bridge this gap, the operational innovation of this study lies in leveraging the combined outputs of high-frequency non-destructive testing (NDT) and millimetric 3D documentation to actively drive the structural detachment and relocation of a severely compromised ancient pavement.

Figure 1. Map of the Marsala area (**left**) and detailed Google Maps view of the investigation zone (**right**), highlighting the Latomia dei Niccolini and the surrounding urban context.

Consequently, this study addresses a fundamental research question: how can high-frequency NDT and close-range photogrammetry be methodologically combined to accurately map subsurface anomalies and safely transform raw diagnostic data into an exact spatial guide for the restoration team? By analyzing the specific case study of the Roman mosaic in the Latomia dei Niccolini, this paper aims to evaluate the precise extent to which integrated digital and geophysical data can mitigate the empirical risks traditionally associated with mosaic lifting, moving beyond a standard technical report toward a replicable, data-driven preservation framework. Specifically, the 3D documentation generated a highly detailed digital model of the surface, essential for planning the physical detachment and restoration steps. Concurrently, the geophysical investigation—assisted by targeted video inspections—determined the exact extension of the surface fractures and the degradation state of the underlying volume. The fusion of these datasets enabled the creation of a three-dimensional geophysical model of the subsoil's electromagnetic reflectivity [2]. This volume proved crucial for reconstructing the geometry of both primary and secondary fractures, as well as for accurately mapping the hidden voids beneath the mosaic floor [3,4]. Ultimately, all the acquired diagnostic information was translated into an operational workflow to successfully execute the physical restoration and relocation of the masterpiece.

2. Geographical and Archaeological Overview of the Research Area

The Latomia dei Niccolini complex consists of ancient open-air stone quarries originally exploited for calcarenite extraction during the peak building expansion of the Roman city of Lilibeum (late 2nd–early 3rd century AD). Located in the south-eastern sector of the urban area of Marsala, adjacent to the municipal cemetery, the site constitutes an integral part of the Archaeological Park of Lilibeo-Marsala (Figure 1). Following its quarrying phase, the site was systematically converted and reused as a hypogeal cemetery complex between the 3rd and 4th centuries AD, forming an extensive subterranean burial nucleus situated between the sacred area of Santa Maria della Grotta [5] and the convent church of Madonna dell'Itria (Odigitria) [6] (Figure 2). The geological matrix is characterized by highly porous local calcarenite, which allowed for rapid rock-cut architecture but poses severe conservation challenges due to its vulnerability to environmental weathering, moisture absorption, and structural mechanical instability.

Systematic archaeological investigations and historical surveys of the sepulchral complexes identified numerous rock-cut features, including arcosolia, niches, and wall niches [7]. Along the eastern front of the Latomia, these excavations highlighted three complexes of arcosolia arranged in Greek-cross and L-shaped plans, seventeen monolithic calcarenite sarcophagi covered with white plaster, and a rock-cut staircase connecting the upper plateau of the ridge with the lower cave structures (Figure 3, modified from [8]). Within this structural layout, the primary focus of conservation is the small southern room, designated as the South cubiculum (or cubiculum 4), which provides access to three specific arcosolia (the "S complex", comprising arcosolia A, B, and C) (Figure 3). The floor of this room houses the fragile polychrome mosaic featuring the kantharos motif. The intensive excavation of these multi-level burial chambers beneath the rocky ridge created a complex system of anthropogenic underground voids, leaving a drastically thinned calcarenite roof layer directly beneath the mosaic preparation bed.

Prior to commencing the non-destructive geophysical and 3D digital surveys, a targeted archaeological cleaning intervention was mandatory to expose the rock-cut layout and analyze the active damage mechanisms (Figure 4a,b). This clearing involved the careful removal of soil deposits and the cutting of extensive root systems that thrived in the damp hypogeal environment, which were actively forcing open the stone joints. In front of the entrance to cubiculum 1 (Figure 4c), the clearing operations highlighted the northern structural extension of the chamber, exposing adjacent cubicula and lithic box tombs that appear to be leaning against and placed in front of the openings of the ancient burial chambers [9]. These include two adjoining box tombs forming part of arcosolium H and an adjacent tomb structure (Figure 4d).

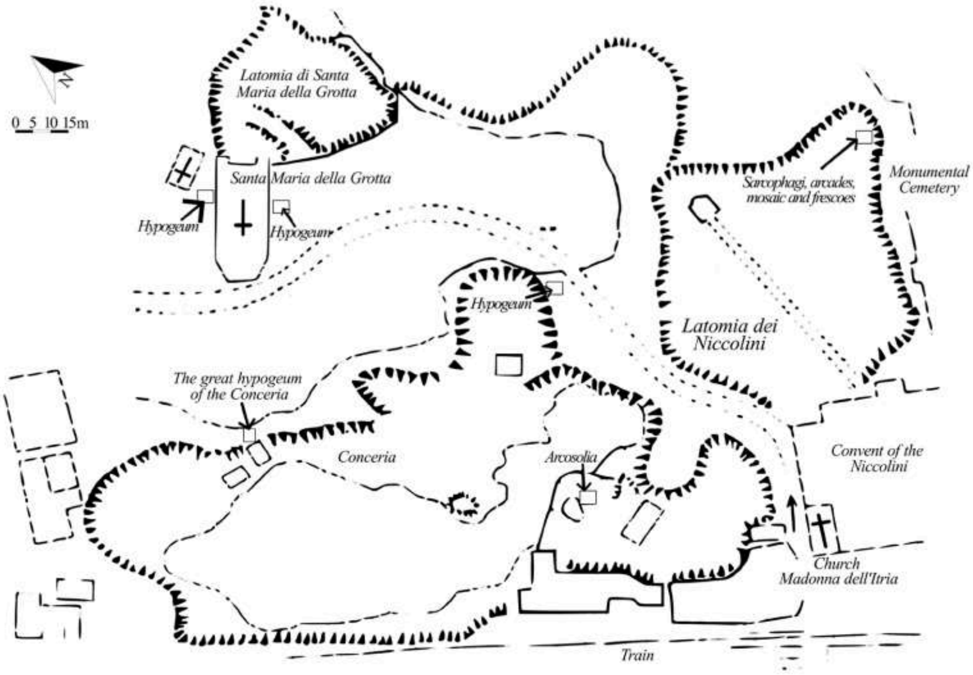

Figure 2. Plan of the Latomia dei Niccolini, Santa Maria della Grotta and Madonna dell'Itria area (modified from [8] by the authors).

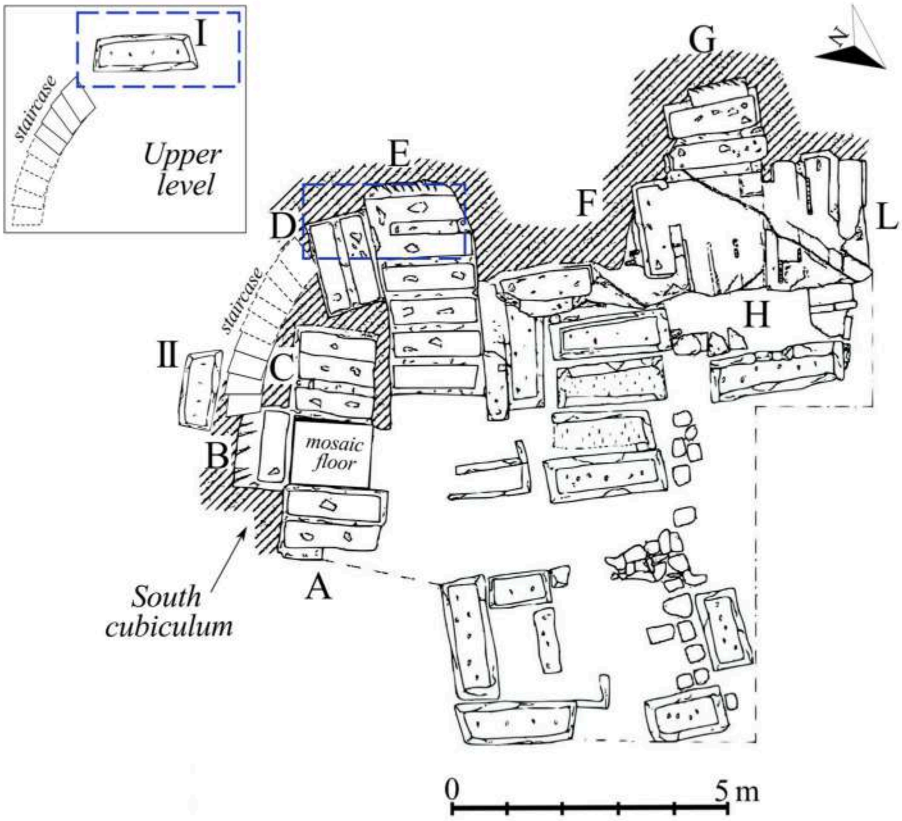

Figure 3. Funerary complex of the Latomia dei Niccolini. The area's arcosolia is illustrated by the letters A–L. The A-B-C arcosolia constitute the "S complex"; D-E are part of the "W complex"; and F-G-H-L are part of the "N-W complex". The arcosolium I, located in the blue dotted rectangle, is situated at the upper level of the burials above the D-E arcosolia, connected by the staircase, while the arcosolium II is located in the lower level near the staircase (modified from [8] by the authors).

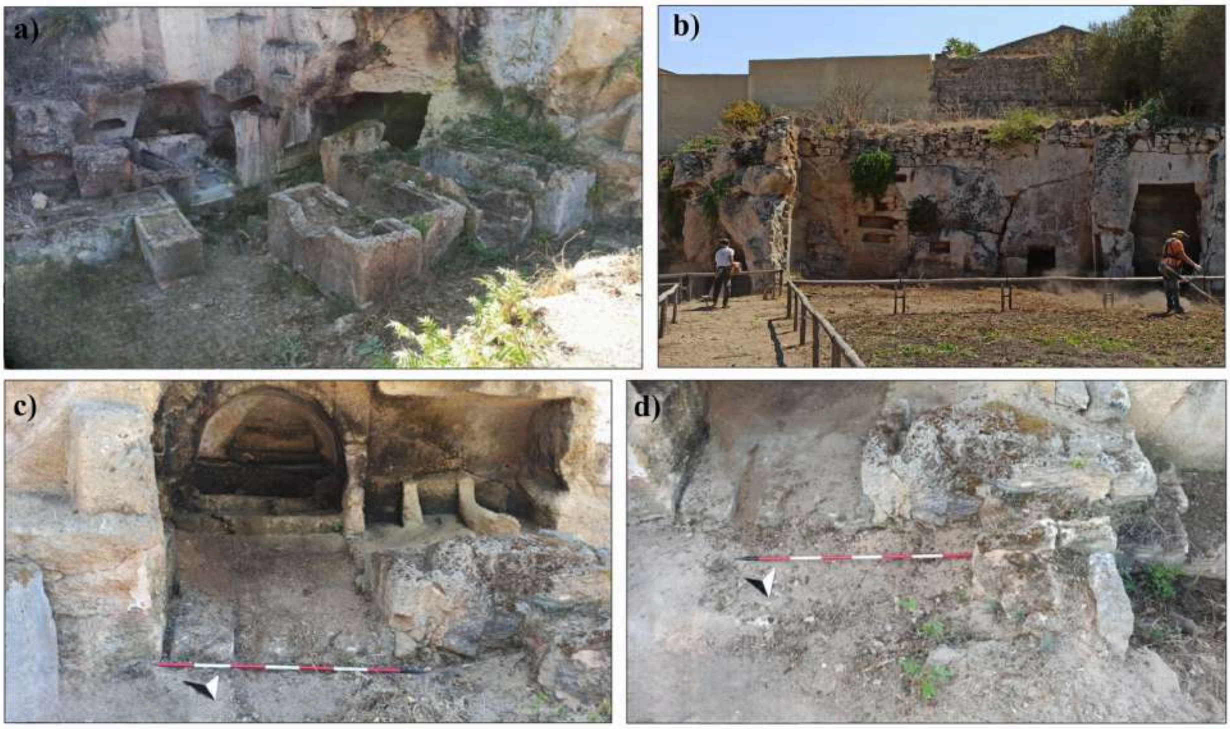

Figure 4. Archaeological site clearing: (**a**) Initial state of the pitch area; (**b**) Clearing; (**c**) Entrance to cubiculum 1 after cleaning; (**d**) Arcosolium H.

In the north-eastern sector, two lithic sarcophagi (approximately 2.20 × 0.77 m), previously documented [10] but reburied over time, were fully uncovered (Figure 5a). The sloping area in front of the cubicula (measuring ca. 4.80 × 5.86 m) was excavated down to the original compacted sandstone pavement (Figure 5b). The removed overburden consisted of humus, ash, and soil deposits highly permeated with modern waste and invasive shrub roots. The presence of these active root systems represents a significant mechanical decay factor for the underlying calcarenite structures.

Figure 5. Archaeological site clearing: (**a**) North-eastern lithic chests after the cleaning; (**b**) Plot area subject to stratigraphic study; (**c**) The entrance stairs to the South cubiculum; (**d**) South cubiculum, arcosolium C after the intervention.

Near the entrance to the South cubiculum, 28 scattered polychrome mosaic tesserae—evidently detached from the main flooring—were recovered alongside the remnants of a plastered stone access structure (Figure 5c). Crucially, the internal cleaning of the South cubiculum provided direct evidence of the structural failures threatening the mosaic. The investigation revealed an alarming cavity between the lower mosaic preparation layer and the underlying earth fill, leaving the pavement severely unsupported. Furthermore, cleaning the adjacent arcosolia (A, B, and C) highlighted severe active subsidence [9]; a major crack in arcosolium A has profoundly compromised the walls and tombs, while arcosolium B was intentionally left filled with earth and stones to prevent further structural yielding of its decorated parapet. Arcosolium C was cleared of extensive roots, soil, and organic debris (Figure 5d), confirming the highly compromised and hollowed nature of the calcarenite supports beneath the mosaic.

Finally, clearing the upper section of the research area revealed the multi-level structural complexity of the rock-cut cemetery. A carved flight of 12 steps (Figure 6a) connects the upper plateau to the lower lay-by, passing adjacent, heavily eroded arcosolia located at higher elevations (Figure 6b,c). This multi-tiered excavation pattern (Figure 6d) visually demonstrates how the intensive hollowing of the rocky ridge created a fragile, multi-level underground network. This complex stratigraphy of voids and thinned rock ceilings establishes the critical geological and structural preconditions for the overlying mosaic's fracture, directly supporting the need for the subsequent diagnostic analysis.

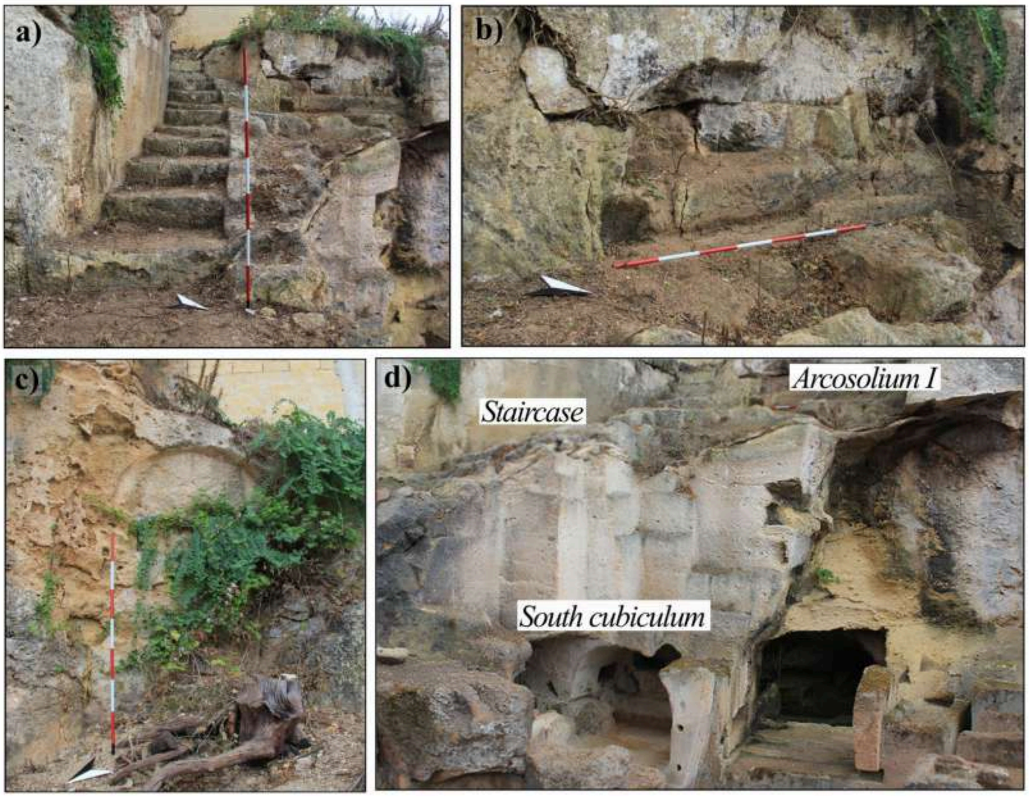

Figure 6. Archaeological site clearing: (**a**) The staircase; (**b**) Arcosolium I; (**c**) Arcosolium II; (**d**) Cemetery entrance hypotheses and different burial levels.

Documenting this surrounding context was essential to establish how the spatial layout of adjacent empty chambers, nearby sarcophagi, and root-induced macro-fissures correlates with the severe differential settlement and diagonal cracking observed on the South cubiculum mosaic floor.

3. Materials and Methods

3.1. Geophysical Investigations by Ground-Penetrating Radar

The ground-penetrating radar (GPR) technique was considered to determine the exact extension of the fracture and the state of degradation of the volume underlying the mosaic of the South cubiculum.

GPR has emerged as a powerful and versatile geophysical technique, revolutionizing the way we investigate and assess archaeological and cultural heritage sites [11–13]. This non-invasive method utilizes electromagnetic waves to penetrate subsurface structures, providing high-resolution images that unveil hidden features without disturbing the site's physical integrity.

In heritage applications, GPR has proven particularly beneficial for mapping archaeological sites, detecting buried structures, and assessing the condition of historical structures without the need for invasive excavation. Its ability to delineate features such as walls, foundations, and even tombs with remarkable precision has significantly enhanced the efficiency and accuracy of archaeological fieldwork [14].

GPR proves to be particularly valuable when it is necessary to investigate subsurface cavities beneath high-value or historically significant flooring, ensuring a non-invasive approach that preserves the integrity of the surface [3,15,16]. In particular, this technique has proven highly effective for the high-resolution characterization of the subsurface layers and the identification of structural anomalies specifically beneath floor mosaics [17,18]. When applied to ancient floorings and Roman mosaics, the technique faces distinct technical challenges due to the micro-stratigraphic nature of the target. A typical historical mosaic structure consists of sub-centimetric decorative elements (tesseratum) overlying thin, multi-layered mortar beds (nucleus, rudus, and statumen). Diagnosing pathologies within these shallow, thin-layer structures—such as localized delaminations, crack propagation, and subsurface voids—requires the deployment of high-frequency antenna systems capable of providing ultra-high vertical and horizontal spatial resolution to isolate the degradation patterns before they trigger surface collapses [19]. In this framework, the multi-sensor integration of high-resolution GPR with close-range photogrammetry has proven to be a highly effective approach for mapping structural decay and monitoring the progression of subsurface air-filled cavities directly beneath Roman mosaic layers [20]. Despite these advancements, thin-bed diagnostics are governed by strict physical constraints, notably the vertical resolution limit defined by the Rayleigh criterion, which dictates that the minimum resolvable thickness of a layer is a quarter of the dominant electromagnetic wavelength [19]. For high-frequency configurations operating in dry mortar contexts, this physical threshold restricts the isolation of overlapping reflections from closely spaced interfaces, making micro-cracks and sub-centimetric delaminations difficult to separate from the dominant structural boundaries of the bedding layers [19]. Furthermore, characterizing the exact geometries of subsurface cracking within highly heterogeneous, multi-layered pavements remains a significant technical challenge that requires advanced electromagnetic velocity calibration and numerical modeling to correlate radar anomalies with real material discontinuities [21]. To overcome these resolution limits and handle signal clutter, modern workflows rely on advanced signal-processing pipelines and advanced imagery techniques. The implementation of microwave tomography and advanced data-processing algorithms has significantly improved the signal-to-noise ratio in cultural heritage surveys, allowing operators to reduce subjectivity during interpretation and successfully reconstruct the three-dimensional geometry of hidden cracks and voids [22]. Additionally, comparative studies on archaeological sites across Italy have highlighted how the combination of 3D amplitude visualizations and advanced signal domain filtering is essential to filter out background stratigraphic noise and successfully isolate critical void networks from ancient restoration patches or structural variances [23].

The selection of GPR as the primary subsurface investigation tool, rather than alternative non-destructive methods such as sonic or ultrasonic testing, was dictated by the extreme fragility and specific conservative status of the mosaic flooring. Although sonic techniques are highly effective for detecting macro-voids, they frequently require direct mechanical coupling or physical contact that exerts acoustic stress on the surface. In this specific archaeological context, such contact could have induced further structural stress, with the additional risk that coupling gels might permanently stain the ancient mortar or porous tesserae. Conversely, high-frequency GPR (using 2 GHz antennas) provides an entirely non-contact, high-resolution spatial mapping capability. This allowed for the continuous tracking of localized subsurface detachments and voids without altering the structural integrity or chemical composition of the mosaic's superficial layers.

3.1.1. Data Acquisition

The GPR investigations were carried out using the IDS Aladdin GPR system (Systems Engineering, 2006). The system consists of a box with two pairs of high-frequency antennas (2 GHz) and a multi-channel DAD central unit capable of managing all IDS antennas. The system is connected to a laptop that manages, displays, and archives the electromagnetic data acquired by the central unit. The use of antennas characterized by a central frequency of 2 GHz (high-frequency) made it possible to obtain a high level of detail in the acquired data.

The profiles were carried out by applying the RSAD (Radar Surface Arrival Detection) sampling technique, configuring the antennas in "bipolar" mode, and sliding them on a plexiglass plate placed in contact with the mosaic, so as not to damage the tiles.

Some preliminary test profiles have been performed to determine the acquisition parameters. Based on the preliminary results, we chose to set up a Butterworth-type bandpass frequency filter for the acquisition, perform horizontal stacking on x traces, and optimize the gain as a function of the round-trip time to compensate for the attenuation of the signal with distance from the source.

The range, which is the recording duration of the signal after each pulse, was set to 14 ns, conservatively, using the formula:

$$Range = 1.5 \times (2D/V), \quad (1)$$

where D is the maximum depth of interest, and V is the average electromagnetic wave velocity through the materials, and 1.5 is a safety factor.

In total, 19 profiles were recorded (Figure 7): 10 along the longest dimension of the mosaic (each approximately 1.4 m long) and 9 orthogonal to the previous profiles and approximately parallel to the shortest dimension of the mosaic (each approximately 0.9 m long).

Figure 7. (**a**) Overview of South cubiculum after clearing; (**b**) View of the floor mosaic, the black arrows are the acquired GPR profiles.

3.1.2. Data Processing

The profiles performed were preliminarily processed using the ReflexW 7.2 software (Sandmeier Geophysical Research, https://www.sandmeier-geo.de/reflexw.html, accessed on 12 May 2026) [24].

Each GPR profile has been processed to eliminate coherent and inconsistent noise present in the original data, following the steps described below [25].

A static correction was applied to correct the time delay in each track. This filter acts on each track individually, allowing time-independent corrections in the tempo direction. We also applied a Butterworth-type frequency filter (frequency range between 150 and 4000 MHz) to eliminate electromagnetic noise with frequencies outside those of the transmitted signal. We then applied an energy decay filter to compensate for the energy losses of the electromagnetic disturbance that occur when the signal propagates through a dissipative medium. This can occur due to various attenuation phenomena, such as the effect of geometrical spreading, dispersion, and transmission losses. This operation serves to emphasize the low-amplitude intervals compared to the higher-amplitude ones, and it does not alter the frequency content of the trace. Finally, we applied the background removal, which consists of subtracting an average trace calculated in a space/time interval chosen in the section on the entire profile, to eliminate constant noises in the space dimension, thus making visible signals that were previously "covered" by the background noises.

To transform the round-trip times of the waves reflected in the depths of the reflectors, we obtained the average velocity of the electromagnetic waves in the medium (and therefore the average relative electrical permittivity ε_r), from the slopes of the branches of the hyperbola in the data and from calibration tests carried out on site. From the value obtained, approximately 0.08 m/ns, the maximum investigation depth reached was estimated, i.e., approximately 0.55 m.

After transforming the time sections into depth sections, the Move 2017.2.0 software suite (Petroleum Experts) was used for 3D spatial georeferencing and volumetric visualization of continuous radar reflections, mapping subsurface anomalies in direct relation to surface coordinates (Figure 8). In this perspective visualization, a selection of the most representative 2D radargrams (B-scans) has been explicitly displayed to support the interpretation of the anomalies; the top-left panel illustrates the complete pseudo-static distribution of the acquired profiles over the mosaic, while the remaining three panels isolate key intersecting B-scans that cross the main damaged areas, clearly revealing the underlying subsurface reflections and signal variations.

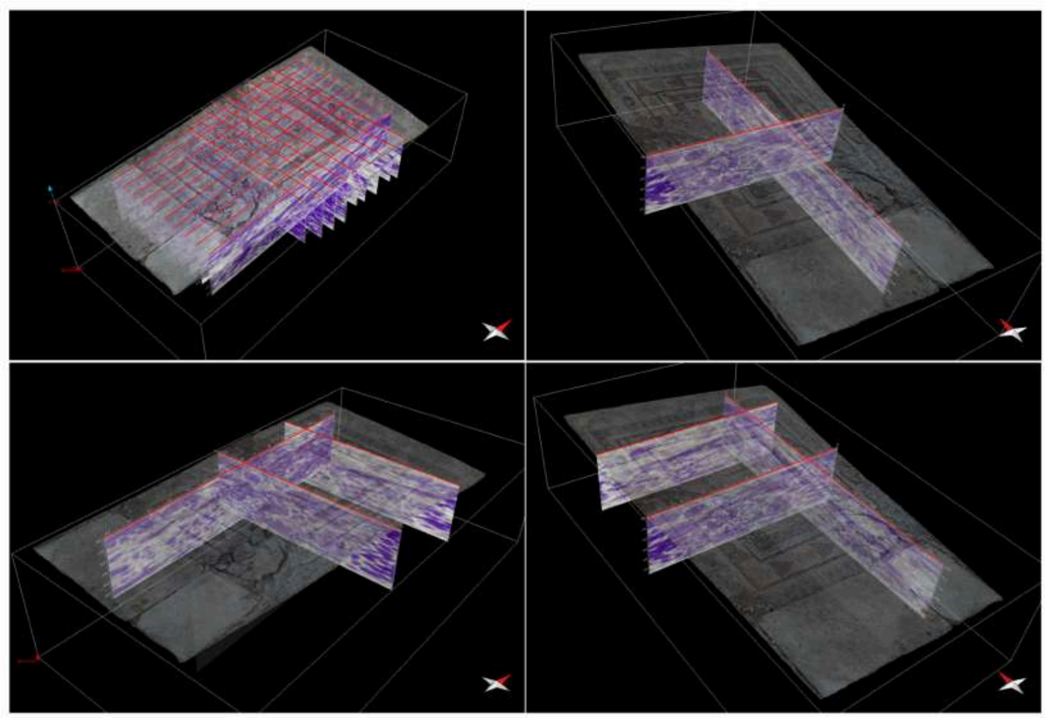

Figure 8. 3D perspective representation of 2D GPR sections (B-scans) beneath the mosaic surface. The top-left panel displays the complete grid of acquired profiles, while the remaining panels isolate the most representative intersecting B-scans showing the main subsurface reflections.

To transform the filtered 2D profiles into an interpretable 3D volume, a Hilbert transform was executed via MATLAB 2024b (MathWorks) to calculate the signal envelope and normalize the electromagnetic amplitude matrix [15,26]. Finally, the three-dimensional data matrix, normalized with respect to its maximum value, was represented using Voxler 4.0 software (Golden Software).

3.2. 3D Survey by Terrestrial Laser Scanner and Close-Range Photogrammetry

In archaeological cultural heritage studies, the geometric knowledge of artifacts is a fundamental prerequisite for historical and archaeological analyses [27]. This becomes even more crucial when studies involve conservation and restoration processes [28].

Three-dimensional survey techniques for archaeological cultural heritage are well-established and have been successfully applied in various contexts, ranging from small and medium-sized object documentation to large-scale archaeological site surveys. Generally, 3D documentation is performed using laser scanner surveys with static or mobile instruments and/or photogrammetric surveys, either terrestrial or aerial [29,30].

The 3D survey of the Latomia dei Niccolini was conducted using a multi-scale approach, initially focusing on the complete 3D documentation of the whole area and subsequently on the detailed documentation of the mosaic undergoing restoration, progressively limiting the area of interest and simultaneously increasing the level of detail in the 3D reconstruction.

3.2.1. 3D Data Acquisition

The initial phase aimed at obtaining a comprehensive 3D reconstruction of the entire site. Due to the site's complexity, given the presence of crevices, niches, and elevated portions, the most appropriate methodology for the survey was based on the use of a mobile laser scanning system [31,32].

The survey was carried out with a Handheld Mobile Laser Scanner (HMLS) GeoSLAM Zeb Horizon RT by GeoSLAM (now FARO Technologies Inc., Lake Mary, FL, USA), which uses Simultaneous Localization and Mapping (SLAM) technology to track the sensor's position and path, enabling the acquisition of a point cloud during the sensor motion. The device has a measurement range of 100 m, an acquisition velocity of approximately 300,000 points per second, and a relative accuracy of $\pm$6 mm. Additionally, the device includes the ZEB Vision system for capturing high-resolution spherical images that allow for RGB registration of the point cloud.

For the acquisition, a single closed-loop trajectory was used to complete the survey, resulting in a point cloud consisting of approximately 88 million points. This point cloud provides an initial 3D reconstruction of the site (Figure 9).

However, due to the occurrence of vegetation at the time of the first survey, the point cloud obtained, despite its high resolution, did not sufficiently allow for the identification and visualization of archaeological structures. Consequently, a second survey was planned and carried out after the archaeological cleaning phase using a static laser scanner to enhance the visibility of the archaeological structures.

The static laser scanner survey focused only on the area surrounding the mosaic of the southern cubiculum, where the most significant archaeological structures are located. The survey was performed using a Faro Focus 3D S120 laser scanner by FARO Technologies Inc., based on phase-shift distance measurement. This instrument has a measurement range of 120 m, an acquisition velocity of 970,000 points per second, and a ranging error of $\pm$2 mm at 10 m and 25 m, each at 90% and 10% reflectivity. The survey was planned to ensure complete coverage and the absence of gaps in the archaeological structures. This was not always achieved as it was not possible to measure the interior of some tombs. A

https://doi.org/10.3390/app16126095

total of eight scans were carried out, with two perimeter scans limiting the horizontal field of view and six full-dome scans performed within the area of interest. The resolutions of the acquisitions ranged from 12 mm at 10 m to 6 mm at 10 m. The use of a static laser scanner provided an extremely detailed point cloud with significantly less noise compared with the mobile laser scanner data (Figure 10).

Figure 9. GeoSLAM Zeb Horizon RT point cloud of the Latomia dei Niccolini.

Figure 10. Faro Focus 3D S120 point cloud of the Latomia dei Niccolini; the gray spheres show the eight scanning positions.

Upon completion of the laser scanning surveys, photogrammetric data acquisition was conducted to generate high-precision 3D models and orthophotos with sub-millimeter accuracy, compatible with a nominal scale of 1:1. The methodology followed the approach used in previous experiments by Lo Brutto and Spera (2016) and Lo Brutto and Dardanelli (2017) [33,34].

The photogrammetric survey was divided into two phases: an initial survey was carried out before the restoration and detachment of the damaged section, and a second survey was performed after the restoration, for both the in situ portion and the fragment preserved in the museum.

A Nikon D5200 camera with a 6000 pixel × 4000 pixel sensor and a fixed focal length Nikon AF-S Nikkor 28 mm lens was used for all the surveys (Nikon, Tokyo, Japan).

The first survey involved acquiring 134 images using stereoscopic and convergent capture schemes from an average distance ranging from 1 m to 1.2 m, achieving an average Ground Sample Distance (GSD) of approximately 0.15 mm. This GSD value is very important for the information and level of detail (even sub-millimetric) that can be detected from the images.

To scale and check the photogrammetric project, five scale bars were used, each equipped with two calibrated distances of 48 and 46 cm, respectively, and appropriately positioned around the area of interest.

The second photogrammetric survey was conducted both in situ, for the mosaic that remained in place, and at the museum for the removed portion of the mosaic.

The survey of the restored in situ mosaic was carried out by acquiring 166 images covering both the mosaic area and the missing section, using the same capture scheme and operational methods as the first survey. In this case, images were obtained with an average GSD of approximately 0.14 mm. The only significant difference compared to the first survey was that it was not possible to position all five previously used scale bars; instead, only four scale bars were used.

The photogrammetric survey of the restored mosaic fragment preserved in the museum was much simpler since the fragment could be positioned most conveniently for image capture. This allowed for a relatively high number of images to be taken, considering the fragment's dimensions (approximately 0.80 m × 0.80 m), from closer distances. Specifically, 162 images were acquired using stereoscopic and convergent capture schemes, from an average distance of about 84 cm, resulting in an average GSD of approximately 0.12 mm. In this case as well, only four scale bars were placed around the mosaic fragment.

3.2.2. 3D Data Processing

The laser scanning data were processed using Autodesk Recap Pro ver. 23.1, following a standard workflow, including importing scans, indexing, point cloud colorization, and automatic registration.

The data acquired with the mobile laser scanner and the static laser scanner were processed within the same project in Recap Pro software. This approach improved the registration process, as the scan performed with the mobile laser scanner covered all parts of the site that were re-acquired with the static laser scanner.

Thanks to the high percentage of overlap between scans and the morphological characteristics of the site, the automatic registration procedure ensured the correct alignment of all scans. The quality assessment of the registration process was performed using both the standard quality parameters provided by Recap Pro software at the end of the registration process (Overlap, Balance, and Points < 6 mm parameters) and qualitative checks on cross-sections of the point clouds. Although this approach is not statistically rigorous, it provides a useful means of assessing the quality of the process.

At the end of this processing phase, the two datasets (one acquired with the GeoSLAM Zeb Horizon RT laser scanner and the other obtained with the Faro Focus 3D laser scanner) were kept separate, resulting in two distinct clusters: the first representing the entire Latomia dei Niccolini area and the second related to the portion closest to the mosaic in the southern cubiculum, where the main archaeological structures are located. This last cluster obtained from the Faro Focus 3D scans was merged into a single point cloud. Using the open-source software CloudCompare ver. 2.13.1, the point cloud was manually segmented to remove all areas outside the zone of interest. Given the acquisition resolutions, the average scanning distances (a few meters), and the high overlap percentage between scans, this point cloud consisted of approximately 15 million points with an average resolution of a few millimeters (~5 mm) (Figure 11).

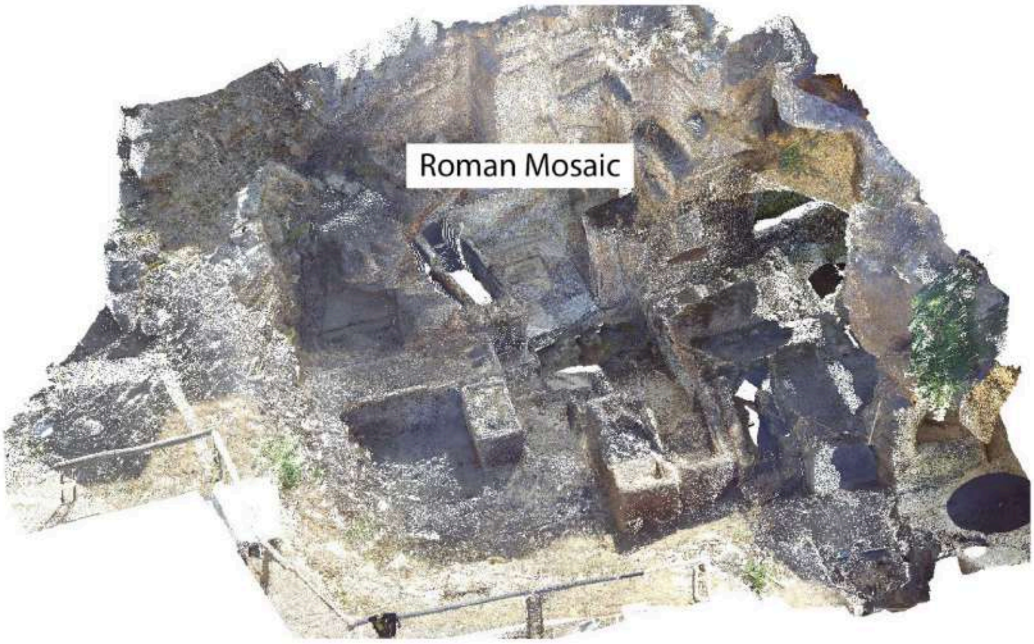

Figure 11. 3D view of the segmented Faro Focus 3D S120 point cloud of the area of interest.

The processing of the photogrammetric surveys was carried out using Agisoft Metashape ver. 2.2.0, following the standard workflow of the software. A single project was created, divided into two distinct sub-projects (referred to as “chunks” in Metashape) for surveying the in situ mosaics, along with a separate project for analyzing the mosaic fragment preserved in the museum. The processing parameters remained consistent across all datasets. The orientation phase, using Structure from Motion (SfM) (known as “alignment” in Metashape), was conducted with the Accuracy parameter set to High and a Tie Point Limit of 4000 points per image (default setting). The subsequent bundle adjustment phase (called “optimization” in Metashape) utilized the 48 cm scale bar distances to scale the project and the 46 cm distances to evaluate the metric accuracy of the image orientation. At the same time, while calculating the external orientation parameters for all images, the internal orientation parameters of the camera were also computed. Specifically, focal length, principal point coordinates, and radial and tangential optical distortion parameters were estimated. The external orientation parameters were assessed based on the residuals calculated from the scale bars present in the project.

After the orientation phase, the point clouds were generated by setting the software’s Quality parameter to Medium. Due to the high resolution of the images, there was no need to generate point clouds with settings that would yield higher resolutions. The next steps involved computing the 3D models of the mosaics (3D mesh), the DEMs, and orthophotos with a resolution of 0.2 mm.

4. Results

4.1. GPR Results

The analysis and interpretation of the GPR data were performed through a three-dimensional representation using Voxler software (Golden Software). To isolate the true geometry of subsurface anomalies from background stratigraphic noise, the radar profiles were processed using a Hilbert transform to extract the instantaneous signal amplitude envelope, with values normalized on a scale from 0 to 1 across the entire dataset. Spatial data interpolation was performed using the Inverse Distance Weighting Method [35], which computes a weighted average based on the distance of the points from the observation point (Figure 12). This workflow yielded volumetric renderings of the subsurface reflectivity, providing a continuous mapping of electromagnetic property variations based on a normalized color scale.

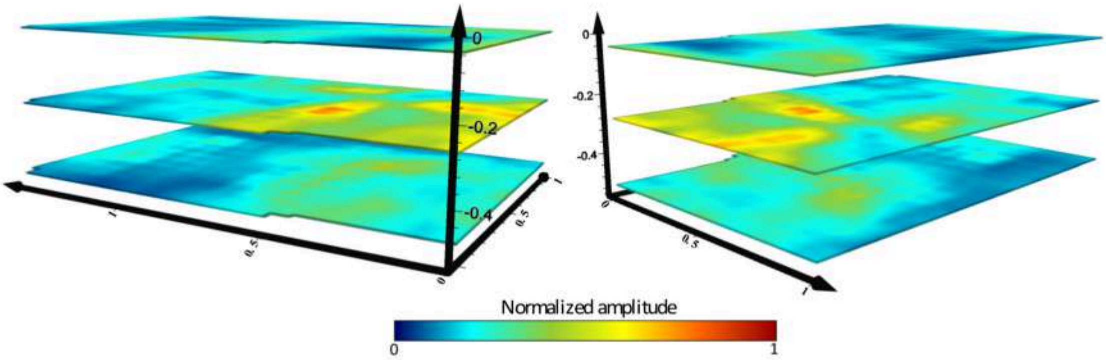

Figure 12. Depth-slice model of subsurface reflectivity beneath the floor mosaic.

The primary purpose of establishing this integrated 3D spatial model was to bridge the gap between superficial structural damage and subsurface geophysical anomalies. By overlaying the high-resolution geometric mesh with the 3D GPR amplitude matrix, the restoration team could visualize the exact geometry and depth of the underground cavity. The practical effect of this model was twofold: first, it prevented catastrophic structural collapses during exploratory micro-drilling and subsequent consolidation phases; second, it provided the precise sub-millimetric topographical data necessary to pre-fabricate a perfectly tailored, lightweight support shell used during the physical detachment and safe transport of the mosaic section.

The resulting 3D volumetric rendering revealed an extensive system of anomalies, where a precise iso-amplitude contour threshold was calibrated to accurately outline the physical boundaries of the hidden cavities. This contour threshold was established at the top 25% of the maximum reflection amplitude (corresponding to normalized values of 0.75 or greater), which defines the solid red isosurface in Figure 13.

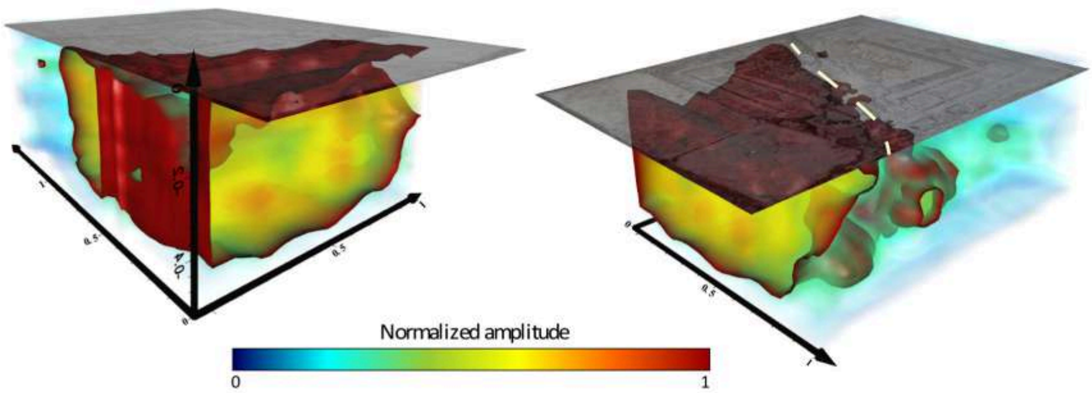

Figure 13. Three-dimensional volumetric rendering of reflection amplitudes under the mosaic floor. The red isosurface marks the region of maximum reflectivity. The white dotted line traces the main surface.

The technical basis for selecting this specific color scale cut-off and threshold relies on the sharp electromagnetic impedance mismatch occurring at the air-to-mortar interface within an underground void. This abrupt physical transition induces maximum phase inversion and peak amplitude reflections of the radar signal. Consequently, filtering the dataset at this threshold allows the software to accurately “outline” and isolate the true spatial extension of the structural voids from the surrounding solid matrix. As visualized, the mapped void system extends in depth to approximately 50 cm and is bounded laterally in strict correspondence with the surface fracture (indicated by the white dotted line in Figure 13), confirming that the structural discontinuity visible on the surface propagates directly downward through the bedding layers.

On the open side of the cubicle, not against the wall, some openings in the underlying masonry allowed a camera inspection to visually investigate the excavations beneath the mosaic. The visual analysis (Figure 14) confirmed, at least in the directly accessible areas, the presence and spatial extent of the cavities; there is a strong correspondence between the high-reflectivity areas and the voids under the mosaic, visible through the side openings.

Figure 14. Video inspection of the South cubiculum subsurface: (**a**) Section view of the entrance area showing the borehole access for the camera; (**b**) View of the cavity under the floor mosaic.

The video inspection images show machined surfaces compatible with an anthropic artefact, the extent of which is mapped by GPR investigations. The anomalies are concentrated mostly in the central portion of the mosaic, which coincides with the structural fracture, while the northern and peripheral sectors are more stable, with no evidence of significant voids or detachments. The 3D GPR model and camera inspection have the same pattern in terms of high-reflectivity areas, confirming the accuracy of the geophysical results.

Overall, integrating 3D GPR modeling with visual inspection enabled a detailed assessment of the mosaic’s substructure. The results show that the cause of surface deformation and fracture may be the gradual subsidence of the voided area beneath the mosaic. This subsidence is likely due to the collapse of the calcarenitic layers or to anthropogenic excavations reused as burial cavities. The identification and precise mapping of these features were crucial for planning the subsequent conservation and stabilization works.

The extraction of quantitative metrics from the integrated datasets provided an objective assessment of the deformation. The multi-scale 3D mesh model quantified the main diagonal fracture with a total continuous length of 130 cm, characterized by a crack opening ranging from 5 to 15 mm and a localized step-fault displacement of about 5 mm. The georeferenced GPR matrix bounded the underlying anomaly to a localized volume with an estimated continuous surface footprint of 4.25 m^2 and a depth range between 5 cm and 40 cm below the tesseratum layer.

4.2. Restoration

The Roman mosaic was in a very critical state of conservation. The collapse affecting the stone floor plan on which it is placed caused, in fact, the big fracture that exposed the mosaic bedding mortar and the limestone below to the rainwater runoff. This physical weathering involved the disaggregation of the mortar and stone and, as a consequence, further cracks, deformations, and the detachment and loss of several tesserae from their bedding (Figure 15a). This situation also resulted in the presence of evident gaps and lacunae.

Figure 15. The initial phase of archaeological restoration: (**a**) The detachment of several tesserae; (**b**) Collection and color classification of erratic tesserae; (**c**) Cleaning the tesserae with water; (**d**) Preliminary dusting.

A conservation treatment of the mosaic was carried out in preparation for the design and construction of a suitable cover and the restoration of the entire cubicle structure. However, to avoid the total loss of the collapsed part of the mosaic, it was planned to detach the fragment and relocate it to a new support, allowing it to be temporarily exhibited at the Regional Archaeological Museum 'Baglio Anselmi' prior to its eventual return to its original location.

The conservation treatment has been preceded by collecting, cleaning with water and classifying by color erratic tesserae (Figure 15b,c). Then, the mosaic was dusted with soft-bristle brushes (Figure 15d). Preliminary dusting was an extremely important operation to understand the degree of adhesion of the tessellation; movable and detached tesserae in their original position were immediately fixed with a weak bedding mortar. Furthermore, the whole floor was disinfected by brushing on a quaternary ammonium salt-based biocide and subsequently rinsed with deionized water.

The removal of the fragment began by covering the surface with cotton gauze adhered using a reversible acrylic resin (Figure 16a). This step protected the tesserae, secured any that might loosen during the operation, and allowed the surface to behave as a single, homogeneous layer. In order to prevent the risk of additional distention of the mosaic rug, the detachment of tessellatum with its preparatory layer was preferred to the lifting of only the tessellatum (Figure 16b).

Figure 16. The archaeological restoration: (**a**) Coating with cotton gauze to carry out the removal of the fragment; (**b**) Detaching of tessellatum; (**c**) Mechanical removal of the deteriorated mortar; (**d**) Application of a new hydraulic mortar; (**e**) Relocation of the mosaic on new support.

The detached mosaic fragment was transported to the museum repository, where mechanical removal of the deteriorated backing mortar (Figure 16c) was carried out using chisels and hammers and micro vibrating pneumatic tools, to proceed with the application of a new hydraulic lime-based mortar similar to the original bedding layer (Figure 16d) and the relocation of the mosaic on a new support. It consisted of a cut-to-measure panel made of an aluminium honeycomb core between two layers of fiberglass-reinforced resin, whose surface was preliminarily treated with a grit-based gripping layer (Figure 16e) fixed with epoxy resin to allow adhesion of the new bedding layer. The millimetric geometric compliance of this custom-built support was ensured by the precise spatial coordinates extracted from the diagnostic models. These coordinates allowed the restoration team to accurately outline the exact perimeter of the detached structural portion south of the fracture, which had an approximately triangular shape with legs measuring 100 cm and 85 cm, and a hypotenuse of 130 cm.

After the mortar had set, the facing fabric was removed one small area at a time by dissolving the adhesive with an appropriate solvent.

After cleaning the surface, it was possible to proceed with stabilizing the mosaic; stabilization aimed to restore the structural stability of the mosaics and prevent any new deterioration from occurring; these procedures also defined the final aesthetic presentation of the conservative treatment.

Resetting tesserae was the first step; detached tesserae were placed back in their original positions and orientations using mortar, guided by a photo of the mosaic at the time of its discovery (Figure 17).

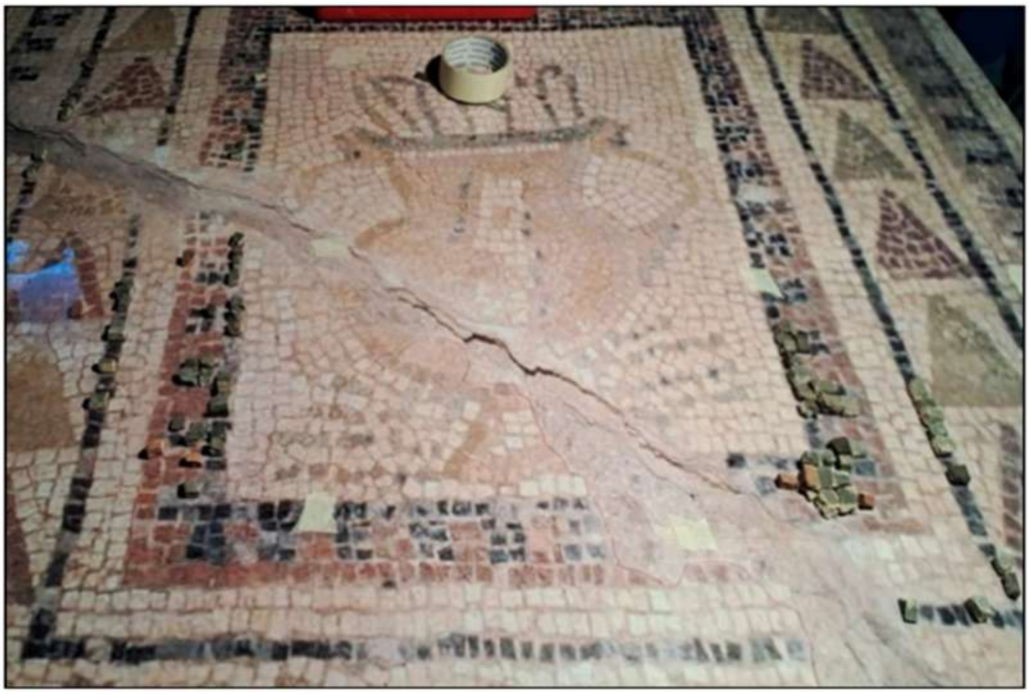

Figure 17. Repositioning the tesserae in their original position, thanks to the photo of the mosaic.

Once the re-adhesion of the tiles was completed, it was possible to establish the real extent of the lacunae. These were small in size and located mainly in the geometric frames; for this reason, a non-consubstantial methodology was adopted for the reconstructions. The filling of lacunae was made by applying mortar replicating the level and chromatic tone of the setting bed of the tesserae (Figure 18a), instead of using similar types of stones [36]. The edges of the section were restrained with the same lime mortar, placed a few millimeters below the level of the preserved mosaic surface. Ultimately, interstices between the tesserae were filled by a liquid lime-based mortar, also called grout, containing very fine aggregates, obtained by sieving the same ones constitutive of the bedding mortar (Figure 18b).

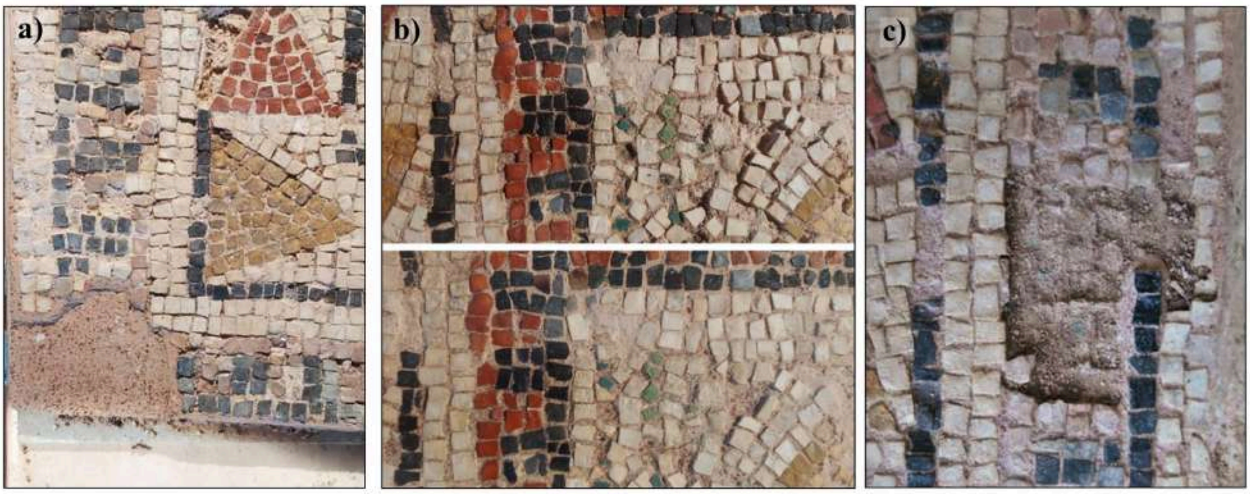

Figure 18. The mosaic's specifics: (**a**) Filling of the gaps with mortar; (**b**) Filling of the interstices between the tesserae with liquid lime-based mortar; (**c**) Imprint of lost tesserae.

Stabilization of the in situ mosaic section, instead, began with the consolidation of the limestone substrate; erosion, in fact, caused powdering and significant loss of original material.

Stone strengthening was obtained by using the lime mortar injection method in order to fill voids and reestablish cohesion among loose calcite grains; reconstructions of missing parts were made with mortar based on hydraulic lime and aggregates similar in appearance and composition to the original stone.

The other stages of work, as the detached, consisted of resetting detached tesserae, consolidating the edges, filing the interstices between tesserae and lacunae, except those in which the original bedding mortar remained and lost tesserae imprints were visible (Figure 18c); in this particular case, it was decided to preserve the archaeological evidence of the executive technique [37].

4.3. 3D Survey Results

The data obtained from the survey were used for precise documentation and the three-dimensional reconstruction of the mosaic before and after the restoration intervention. This made it possible to conduct an objective analysis of the various work steps and provided essential documentation for future mosaic monitoring operations.

Using the tools available in Metashape software, the two chunks of the photogrammetric survey project for the in situ mosaic were brought into the same reference system. The alignment of the two chunks was performed by identifying homologous points in the two sub-projects (Marker-based method). This approach allowed for the perfect alignment of the two orthophotos, enabling detailed verification of all restoration interventions. Thanks to the high geometric resolution of the orthophotos (0.2 mm) and the precise data correspondence, it was possible to examine the work carried out on each tessera (Figure 19). This operation was also performed on the 3D models; Figure 20 shows the overlay of the two 3D models before and after restoration.

Additionally, a virtual relocation of the removed mosaic fragment was tested to virtually reconstruct the entire restored mosaic. This operation was performed by identifying the coordinates of three points in the removed section of the mosaic within the pre-restoration Metashape project and using these coordinates to apply a roto-translation to the Metashape project of the fragment. In this way, both the orthophoto and the 3D model of the mosaic fragment were brought into the same reference system used for the in situ portion. This allowed for a semi-rigorous reconstruction of the fragment's position (Figure 21).

Although this methodological approach could be considered highly rigorous due to its reliance on identifying common points, in our case, it is classified as semi-rigorous because the estimated positions of the in situ points are affected by deformations resulting from the collapse of the mosaic floor. Therefore, the positions of the points from the in situ mosaic cannot be considered perfectly corresponding to those in a restored mosaic where the surface has been leveled. Despite these limitations, the chosen approach remains the most accurate way to achieve the desired outcome.

It is also quite evident that the virtual reconstruction of the mosaic is influenced by the absence of smaller fragments along the fracture line. These portions were not relocated because they were either severely damaged or entirely missing.

The subsequent virtual reconstruction process was carried out by overlaying the 3D model of the mosaic onto the 3D model of the site. This operation was made by registering the mosaic point clouds with the laser scanner point cloud in CloudCompare. This allowed for the digital 3D reconstruction of the area before and after the restoration of the mosaic (Figure 22).

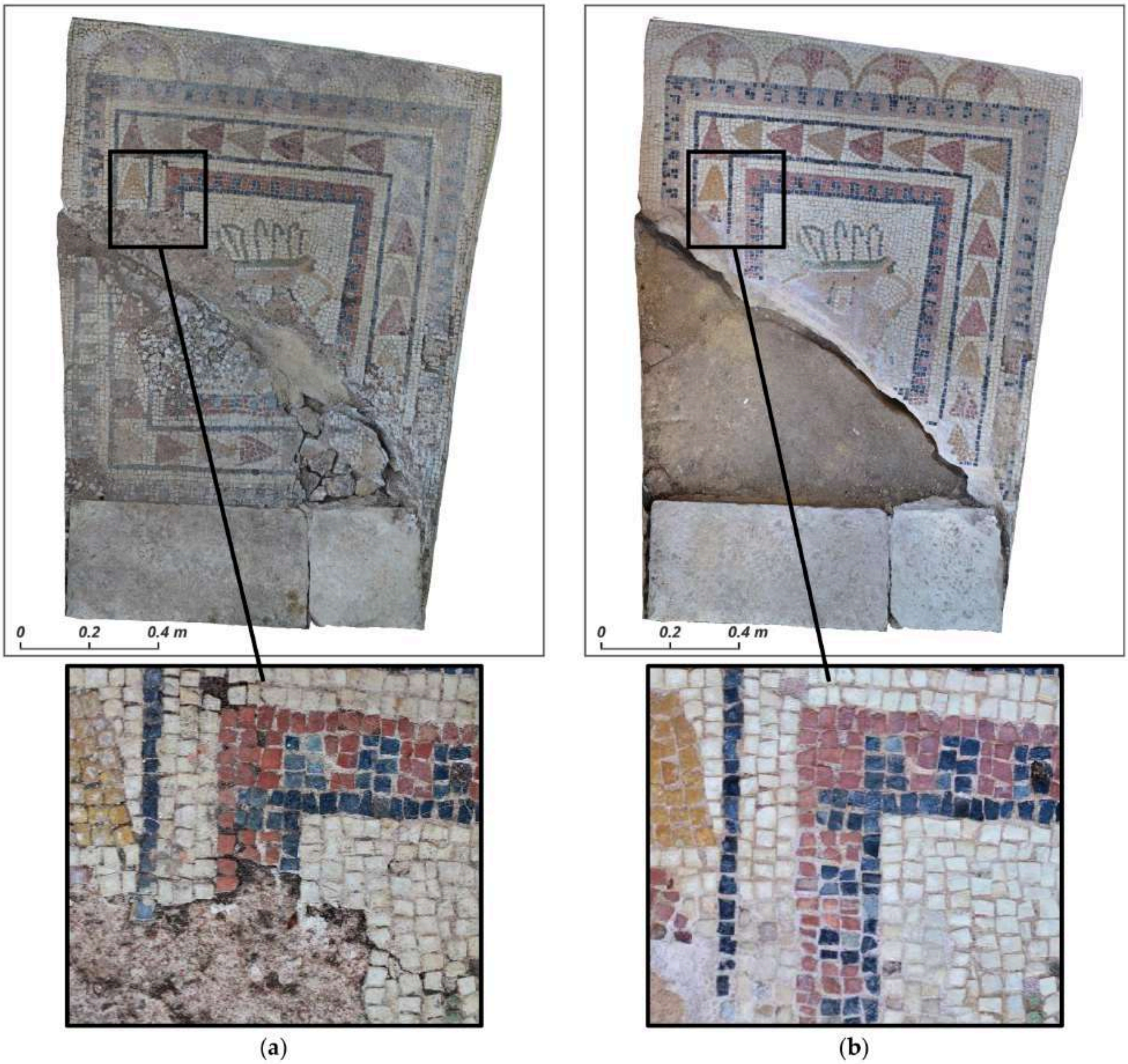

Figure 19. Orthophotos of the mosaic of the South cubiculum: (**a**) Before restoration process; (**b**) After restoration process.

Figure 20. View of 3D models of the mosaic before (**on the left**) and after (**on the right**) restoration.

Figure 21. View of the orthophoto of the mosaic in situ after restoration with virtual relocation of the removed and restored fragment.

Figure 22. 3D reconstruction of the site: (**a**) before the restoration of the mosaic; (**b**) after the restoration of the mosaic.

5. Discussion

The interdisciplinary methodology adopted in this study, integrating non-invasive geophysical prospecting with high-resolution 3D documentation and traditional archaeological restoration, proved highly effective for the conservation of the Roman mosaic in the Latomia dei Niccolini. This holistic approach allowed for a comprehensive assessment of the site, effectively mitigating the gap between visible surface degradation and the underlying structural causes.

Specifically, the application of GPR provided critical insights into the subsurface features and structural integrity of the mosaic floor's subsurface features and structural integrity in the South cubiculum floor in the South cubiculum. The 3D volumetric rendering of the GPR data revealed a complex network of high-reflectivity anomalies, interpreted as structural voids, extending to a depth of approximately 50 cm. These anomalies were not randomly distributed but were particularly concentrated in the area corresponding to the main diagonal fracture on the surface. This correlation strongly suggests that the surface deformation was driven by the progressive subsidence of the underlying calcarenite layers and the presence of anthropogenic cavities used for burials. These geophysical findings were consistently validated by direct visual inspections conducted via a well camera, which confirmed the presence and extent of the voids. The convergence of geophysical data and visual evidence underscores the reliability of GPR as a primary non-destructive diagnostic tool for assessing structural pathologies in fragile archaeological contexts.

Concurrently, the multi-scale 3D survey, combining laser scanning and close-range photogrammetry, was fundamental not only for documentation but also for operational planning. The integration of mobile and static laser scanning provided a complete geometric framework of the complex hypogeal environment, while high-resolution photogrammetry (with a GSD of ~0.2 mm) generated accurate digital twins of the mosaic floor. These 3D models served a dual purpose: they provided a rigorous metric record of the artifact's state before intervention and supported the complex operations of detachment and virtual reconstruction. The ability to align and overlay the pre- and post-restoration orthophotos offered an objective method to verify the positioning of the detached fragment and to monitor the stability of the remaining in situ portions over time.

The diagnostic data directly informed the conservation strategy, ensuring that interventions were targeted and technically justified. Specifically, the decision-making threshold for executing the physical detachment of the mosaic flooring was mathematically driven by the spatial intersection of surface and subsurface risk parameters. Intervention became mandatory because the close-range photogrammetric model recorded a surface crack width exceeding 5 mm, coupled with a vertical displacement of about 5 mm. Crucially, the 3D GPR matrix mapped a continuous, completely unsupported subsurface cavity at a depth ranging from 5 to 40 cm directly beneath that exact crack, covering a continuous area of over 4 m^2. This spatial relationship meant that the compromised mosaic layer was effectively "suspended" in mid-air. Under these structural configurations, in situ consolidation via fluid mortar or resin injection was rejected due to the high risk of structural collapse and uncontrolled material dispersion into the underlying hypogeum structures, thereby dictating the absolute necessity of localized physical detachment. Following this data-driven decision, the restoration process, which included surface cleaning, the removal of erratic tesserae, biocide application, and substrate consolidation, successfully mitigated the immediate risks of material loss. Furthermore, the relocation of the detached fragment onto a lightweight aluminium honeycomb support ensures its physical preservation and reversibility, allowing for its temporary exhibition at the Regional Archaeological Museum 'Baglio Anselmi' and facilitating its future reinstallation in situ.

6. Conclusions

This study evaluated the integration of high-frequency GPR and 3D photogrammetric surveying as a methodological framework for the structural conservation of vulnerable Roman mosaics, addressing the primary research question regarding risk mitigation during physical interventions. The application of these non-destructive techniques allowed for the characterization of specific structural pathologies, specifically the subsidence of the bedding layers, without inducing mechanical stress on the fragile surface. The resulting subsurface anomaly maps provided the restoration team with precise spatial boundaries, which guided the localized detachment process and minimized the loss of original material.

The correlation between superficial 3D data and subsurface geophysical model enabled the mapping of the underlying void system and its relationship with surface fractures. This diagnostic output provided the technical justification for detaching the compromised mosaic section, which was subsequently consolidated and transferred onto a lightweight, reversible aluminum honeycomb support. This procedure ensured the physical stability of the artifact for its temporary display at the Regional Archaeological Museum 'Baglio Anselmi', while fulfilling the conservation requirement of reversibility for potential future reinstallation in situ.

The applied methodology presented distinct advantages: the non-contact nature of the GPR survey ensured total surface preservation during the diagnostic phase, while the subsurface anomaly maps provided the restoration team with precise spatial boundaries, directly optimizing the localized detachment process and minimizing the loss of original material. However, some limitations must be acknowledged. GPR data interpretation remains highly complex and operator-dependent when dealing with highly heterogeneous archaeological strata, damp environments, or multi-layered historical reconstructions, which can attenuate electromagnetic signals and cause reflections that are difficult to isolate.

To address the inherent interpretation complexities and operator dependency associated with GPR data in heterogeneous and damp archaeological strata, future research should focus on two main axes. First, the development of automated data-processing pipelines and machine learning algorithms is required to reduce subjectivity in radargram analysis. Second, the generated 3D models will be utilized for multi-temporal structural monitoring to assess the long-term stability of the remaining in situ structures and track potential structural settlements of the relocated mosaic sections over time.

Author Contributions: Conceptualization, P.C., R.M. and M.L.B.; methodology, P.C., R.M. and M.L.B.; software, A.C. (Alessandra Carollo) and M.L.B.; validation, A.C. (Alessandra Carollo), R.M. and M.L.B.; formal analysis, A.C. (Alessandra Carollo), A.C. (Angelina Castiglia). and M.L.B.; investigation, A.C. (Alessandra Carollo), P.C., R.M., A.A., A.C. (Angelina Castiglia) and M.L.B.; resources, R.M. and M.L.B.; data curation, A.C. (Alessandra Carollo) and M.L.B.; writing—original draft preparation, A.C. (Alessandra Carollo), A.A., A.C. (Angelina Castiglia) and M.L.B.; writing—review and editing, A.C. (Alessandra Carollo), R.M. and M.L.B.; visualization, P.C.; supervision, R.M.; project administration, R.M. All authors have read and agreed to the published version of the manuscript.

Funding: This research received no external funding.

Institutional Review Board Statement: Not applicable.

Informed Consent Statement: Not applicable.

Data Availability Statement: Data can be obtained upon request from the corresponding author.

Acknowledgments: The authors would like to acknowledge Anna Vincenza Occhipinti, Director of the Archaeological Park of Lilibeo, for granting access to the site and for her institutional support. Sincere thanks are extended to Maria Grazia Griffo for her valuable scientific advice and contribution to the study. The authors also gratefully acknowledge the "Amici del Parco di Lilibeo" Association for the technical and logistical support provided during the planning and execution of the mosaic detachment, as well as for its relocation to the Regional Archaeological Museum "Baglio Anselmi".

Conflicts of Interest: Author Angelina Castiglia was employed by the company PROPERART Cooperative Company. The remaining authors declare that the research was conducted in the absence of any commercial or financial relationships that could be construed as a potential conflict of interest.

References

1. Ercoli, L.; Zimbardo, M.; Nocilla, A. Rock decay phenomena and collapse processes in the "Latomiae del Paradiso" in Syracuse (Sicily). *Eng. Geol.* **2014**, *178*, 155–165. [CrossRef]
2. Daniels, D.J. *Ground Penetrating Radar*, 2nd ed.; Institution of Electrical Engineers: London, UK, 2004. [CrossRef]
3. Capizzi, P.; Martorana, R.; Messina, P.; Cosentino, P.L. Geophysical and geotechnical investigations to support the restoration project of the Roman 'Villa del Casale', Piazza Armerina, Sicily, Italy. *Near Surf. Geophys.* **2012**, *10*, 145–160. [CrossRef]
4. Martorana, R.; Capizzi, P. Joint Investigation with Ground Penetrating Radar and Infrared Thermography as a Diagnostic Support for the Restoration of Two Wall Mosaics in the Church of St. Mary of the Admiral in Palermo, Italy. *Heritage* **2022**, *5*, 2298–2314. [CrossRef]
5. Abrignani, A. Il monachesimo siculo-greco nel territorio di Marsala: Fonti e topografia. In *VI Ciclo di Studi Medievali (Firenze, 8–9 Giugno 2020)*; Gruppo di Ricerca sul Medioevo Latino NUME: Lesmo, Italy, 2020; pp. 54–59.
6. Lombardo, D.; Pappalardo, C. Il palinsesto pittorico della chiesa di Santa Maria dell'Itria a Marsala. In *VI Ciclo di Studi Medievali. Atti del Convegno (Firenze, 8–9 Giugno 2020)*; Gruppo di Ricerca sul Medioevo Latino NUME: Lesmo, Italy, 2020; pp. 259–264.
7. Führer, J.; Schultze, V. *Die Altchristlichen Grabstätten Siziliens*; Forgotten Books: Berlin, Germany, 1907.
8. Vecchio, P. L'area archeologica dei Niccolini. In *Da Lilibeo a Marsala*; Griffo, M.G., Ed.; Regione Siciliana, Assessorato dei Beni Culturali e dell'Identità Siciliana: Palermo, Italy, 2010; Volume 4, pp. 27–29.
9. Abrignani, A. L'area cimiteriale del Complesso dei Niccolini di Lilibeo (Marsala, TP): Nuove osservazioni e riletture. In *Archeologia Cristiana in Italia. Ricerche, Metodi e Prospettive (1993–2022)—Atti del XII Congresso Nazionale di Archeologia Cristiana (Roma, 20–23 Settembre 2022)*; Braconi, M., David, M., Fiocchi Nicolai, V., Nuzzo, D., Spera, L., Stasolla, F.R., Eds.; SAP: Quingentole, Italy, 2024; Volume II, pp. 983–994.
10. Giglio, R. Lilibeo (Marsala): Nuove scoperte archeologiche nell'area di Santa Maria della Grotta e del complesso dei Niccolini. In *Sicilia Archeologica XXX*; Ente Provinciale per il Turismo di Trapani: Trapani, Italy, 1997; pp. 45–58.
11. Cozzolino, M.; Di Giovanni, E.; Mauriello, P.; Piro, S.; Zamuner, D. *Geophysical Methods for Cultural Heritage Management*; Springer: Berlin/Heidelberg, Germany, 2018; p. 211. [CrossRef]
12. Barone, P.M.; Ruffell, A.; Tsokas, G.N.; Rizzo, E. Geophysical Surveys for Archaeology and Cultural Heritage Preservation. *Heritage* **2019**, *2*, 2814–2817. [CrossRef]
13. Martorana, R.; Capizzi, P.; Pisciotta, A.; Scudero, S.; Bottari, C. An Overview of Geophysical Techniques and Their Potential Suitability for Archaeological Studies. *Heritage* **2023**, *6*, 2886–2927. [CrossRef]
14. Goodman, D.; Piro, S. *GPR Remote Sensing in Archaeology*; Springer: Berlin/Heidelberg, Germany, 2013; Volume 9, p. 233. [CrossRef]
15. Bottari, C.; Capizzi, P.; Martorana, R.; Azzaro, R.; Branca, S.; Civico, R.; Fucile, M.; Pecora, E. Diagnostic Multidisciplinary Investigations for Cultural Heritage at Etna Volcano: A Case Study from the 1669 Eruption in the Mother Church at the Old Settlement of Misterbianco. *Remote Sens.* **2022**, *14*, 2388. [CrossRef]
16. Martorana, R.; Capizzi, P. Seismic and non-invasive geophysical surveys for the renovation project of Branciforte Palace in Palermo. *Archaeol. Prospect.* **2023**, *30*, 13–26. [CrossRef]
17. Calia, A.; Leucci, G.; Masini, N.; Matera, L.; Persico, R.; Sileo, M. Integrated prospecting in the crypt of the Basilica of Saint Nicholas in Bari, Italy. *J. Geophys. Eng.* **2012**, *9*, 271–281. [CrossRef]
18. Calia, A.; Lettieri, M.; Leucci, G.; Matera, L.; Persico, R.; Sileo, M. The mosaic of the crypt of St. Nicholas Bari (Italy): Integrated GPR and laboratory diagnostic study. *J. Archaeol. Sci.* **2013**, *40*, 4162–4169. [CrossRef]
19. Negri, S.; Aiello, M.A. High-resolution GPR survey for masonry wall diagnostics. *J. Build. Eng.* **2021**, *43*, 102545.
20. Lachhab, A.; Benyassine, E.M.; Atki, M. Integration of laser level survey, photogrammetry and GPR to examine the deterioration of Roman mosaics: A case study of Venus house, Volubilis, Morocco. *Archaeol. Prospect.* **2023**, *30*, 14–25.
21. Rasol, M.A.; Pérez-Gracia, V.; Fernandes, F.M.; Pais, J.C.; Santos-Assunçao, S.; Sossa, V. GPR laboratory tests and numerical models to characterize cracks in cement concrete specimens, exemplifying damage in rigid pavement. *Measurement* **2020**, *158*, 107696. [CrossRef]
22. Catapano, I.; Gennarelli, G.; Ludeno, G.; Soldovieri, F. Applying ground-penetrating radar and microwave tomography data processing in cultural heritage: State of the art and future trends. *IEEE Signal Process. Mag.* **2019**, *36*, 53–61. [CrossRef]
23. Piro, S.; Campana, S. GPR investigation in different archaeological sites in Tuscany (Italy). Analysis and comparison of the obtained results. *Near Surf. Geophys.* **2012**, *10*, 429–440. [CrossRef]
24. Sandmeier, K.J. *ReflexW, Version 8.1. Program for Processing of Seismic, Acoustic or Electromagnetic Reflection, Refraction and Transmission Data*; Software Manual; Sandmeier Software: Karlsruhe, Germany, 2016.
25. Cassidy, N.J. Ground Penetrating Radar Data Processing, Modelling and Analysis. In *Ground Penetrating Radar Theory and Applications*; Jol, H.M., Ed.; Elsevier: Amsterdam, The Netherlands, 2009; pp. 141–176. [CrossRef]
26. Capizzi, P.; Martorana, R.; Canzoneri, A.; Carollo, A.; Majani, M.V. 3D GPR Model in the Military District of San Giacomo Degli Spagnoli (Palermo). *Heritage* **2023**, *6*, 2601–2613. [CrossRef]

27. Barrile, V.; Gattuso, C.; Genovese, E. Review of Geomatics Solutions for Protecting Cultural Heritage in Response to Climate Change. *Heritage* **2024**, *7*, 7031–7049. [CrossRef]
28. Croce, V.; Caroti, G.; Piemonte, A.; Bevilacqua, M.G. Geomatics for Cultural Heritage conservation: Integrated survey and 3D modelling. In Proceedings of the International Conference on Metrology for Archaeology and Cultural Heritage, MetroArchaeo, (IMEKO TC-4), Florence, Italy, 4 December 2019; pp. 217–276.
29. Fernández-Hernandez, J.; González-Aguilera, D.; Rodríguez-Gonzálvez, P.; Mancera-Taboada, J. Image-based modelling from UAV photogrammetry: An effective, low-cost tool for archaeological applications. *Archaeometry* **2015**, *57*, 128–145. [CrossRef]
30. Verykokou, S.; Ioannidis, C. An Overview on Image-Based and Scanner-Based 3D Modeling Technologies. *Sensors* **2023**, *23*, 596. [CrossRef] [PubMed]
31. Aricò, M.; La Guardia, M.; Lo Brutto, M.; Rappa, E.M.; Vinci, C. Mobile Mapping for Cultural Heritage: The Survey of the Complex of St. John Hermits Palermo (Italy). *Int. Arch. Photogramm. Remote Sens. Spat. Inf. Sci.* **2023**, *48*, 25–32. [CrossRef]
32. Teppati Losè, L.; Rinaudo, F.; Grasso, N.; Bonfanti, C.; Kappes, S. Moving Toward the Next Generation of HMLS—Testing and Validating the Performances of Second-Generation SLAM Systems Compared to Predecessors. *Sensors* **2025**, *25*, 2488. [CrossRef] [PubMed]
33. Lo Brutto, M.; Spera, M.G. 3D mosaics survey: Analysis of photogrammetric/computer vision approach in a metrological context. In Proceedings of the IMEKO International Conference on Metrology for Archaeology and Cultural Heritage, Torino, Italy, 19–21 October 2016; pp. 185–190.
34. Lo Brutto, M.; Dardanelli, G. Vision metrology and Structure from Motion for archaeological heritage 3D reconstruction: A Case Study of various Roman mosaics. *Acta Imeko* **2017**, *6*, 35–44. [CrossRef]
35. Shepard, D. A two-dimensional interpolation function for irregularly-spaced data. In *Proceedings of the 1968 23rd ACM National Conference*; Association for Computing Machinery: New York, NY, USA, 1968; pp. 517–524. [CrossRef]
36. Nardi, R.; Zizola, C.; de Guichen, G. Il mosaico del monastero di Santa Caterina nel Sinai: Riflessioni sul trattamento delle lacune. In *Miscellanea in onore di Federico Guidobaldi*; Pontificio Istituto di Archeologia Cristiana: Città del Vaticano, 2011.
37. Perpignani, P. Mosaico pavimentale con emblema detto 'dei pugili'. In *RESTITUZIONI 2016. Tesori d'Arte Restaurati*; Bertelli, C., Bonsanti, G., Eds.; Marsilio: Venezia, Italy, 2016; pp. 56–61. Available online: http://restituzioni.marsilioeditori.it/2016/docs/Restituzioni_2016_catalogo.pdf (accessed on 13 May 2026).